Modeling and Designing of a Drift-free Biocompatible Pressure Sensor for use in Long Term In-Vivo testing

University of Illinois at Chicago - NSF REU Summer 2010:
REU Student: Sagar Nadimpalli (snadim3@uic.edu)
REU Advisor: Dr. Alan Feinerman (feinerman@uic.edu)
REU Graduate Student Advisor: Mr. Kasun Punchihewa (kpunch2@uic.edu)
8-6-2010

Modeling and Designing of a Drift-free Biocompatible Pressure Sensor for use in Long Term In-Vivo testing

S. Nadimpalli[1], K. Punchihewa[2] and A. Feinerman[2]

[1]Department of Bioengineering, University of Illinois at Chicago, Chicago, IL 60607
[2]Department of Electrical and Computer Engineering, University of Illinois at Chicago, Chicago, IL 60607

Abstract

Recent medical practice indicates the need for an appropriate pressure monitoring device to combat medical situations such as brain hemorrhages and glaucoma. A significant pressure change of around 10 Torr or more can result in an interference of the blood flow. The purpose of this project was to model, design and test a drift-free biocompatible pressure sensor prototype which measures small variations in pressure within a closed chamber. This can lead to future medical applications during treatments such as an implanted body pressure sensor. To measure the impedance variation of the sensor with changes in pressure and salt concentrations, the prototype underwent three tests: Changing the pressure and studying how the impedance was influenced accordingly; Variations of the impedance based on the salt concentration amount that it was placed into over a certain period of time; Change of pressure in order for monitoring the variation in conductivity.

Key Words: *Pressure Sensor, Mylar, Pressure, Impedance, Conductivity, LDPE*

Introduction

The use of pressure sensors have been studied extensively in situations for which an appropriate pressure monitoring system is required for clinical applications such as glaucoma or hemorrhages. Glaucoma is the situation known where there is a buildup of pressure in the eye which can lead to potential blindness if it progresses to that stage. The excess buildup of pressure due to fluid causes damage to the optic nerve.[1, 5-6] Through various modeling and experimentation, a relationship has been established between the pressure between two nodal points of a blood vessel and the flow through that region has been shown to be directly proportional. So if the blood flow pattern happens to get disturbed by for instance a significant change of 10 Torr or more, the flow through that region can be affected. This can be of important significance if the flow does not get through with a major drop in pressure. The other situation that we can consider is the build-up of pressure causing an overflow of the fluid if it cannot flow through as such.[2]

For these experiments, an appropriate drift-free biocompatible pressure sensor will be fabricated and tested. The first step of this project is the design and fabrication of this sensor. Once complete the prototypes will be tested in-vitro in a custom built vacuum chamber. After successful testing of the prototypes, fabrication of the actual scale sensors will begin. In respect to an appropriate drift-free biocompatible substance, we are possibly considering vaseline and other substances that would be good potential tests to cover the sensor and monitor whether the device drifts or not accordingly. With the selected design material, the situation of biocompatibility shall have been handled. Eventually, we would implant three pressure sensors into laboratory rabbits to test for

biocompatibility. Once that has occurred successfully, we plan to test the sensor's capabilities in various regions of the rabbit.[1, 3]

In this experiment, an appropriate biocompatible pressure sensor will be designed using metalized thermoplastic polyester films with a substance known as Mylar, and low-density polyethylene (LDPE) as central tubing and as a cover for the electrodes. The electrodes are made of titanium based alloy metals consisting of the following: 90% Titanium, 6% Aluminum, and 4% Vanadium. This is important to note because other materials have been looked for as well as cheaper alternatives. It has been noted through various experimentations in the past at our lab that stainless steel was once thought of as a possibility. However, this material has known to cause potential interference issues during MRI procedures. It has been indicated that the previously listed materials are biocompatible.[3] Finally, a saline-form based solution is used [not saline actually] known as the BSS (Balanced Salt Solution). It contains mainly 0.64% of sodium chloride and 0.075% of potassium chloride per 1 ml of this BSS material.

Two Mylar films are welded together using a vacuum which creates a compliant thermoplastic fluid reservoir. Following this, two LDPE covered electrodes along with a 30 cm LDPE tube are welded into the inside of this compliant thermoplastic fluid reservoir. Next, a positive gauge pressure gets applied upon the sack fluid which drains into the reservoir resulting in a compression of a small air column. This contraction of the reservoir will result in a change in electrical impedance. These impedance readings can be correlated as an applied pressure which therefore signifies that an accurate intraocular pressure reading can be read.[4]

Fig. 1: A pressure sensor. Compliant liquid reservoir is made of Mylar film with a central LDPE tube to place the compliant liquid (saline) into at the middle and LDPE electrodes inserted into the outer edges of the film.

.

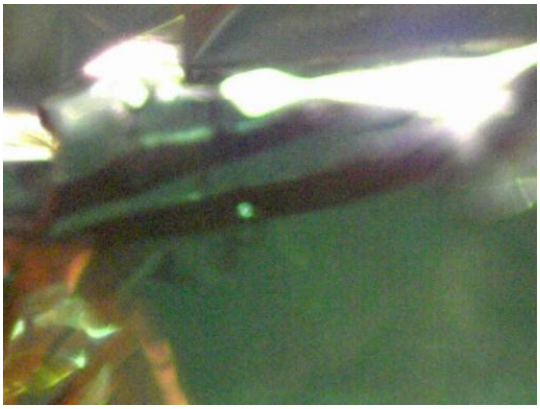

Fig. 2: 60x magnification of compliant liquid reservoir of prototype sensor. Two circular LDPE electrodes are located on the outer edge of the fluid sack. The separation of the two electrodes can be seen in the upper right corner.

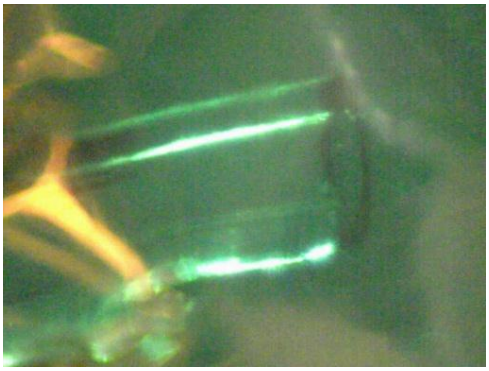

Fig. 3: 60x magnification of LDPE rigid gas reservoir in prototype sensor. The Fluid-gas interface is located in the center of the image. This interface will advance or recede with varying applied pressure.

The strategy to handle the novel process of welding thermoplastic films together using a vacuum frame and carbon dioxide laser has been designed in Dr. Feinerman's laboratory at UIC. This procedure allows us to create leak proof welds and fluid channels in Mylar films.[1, 4]

Methods

Part I: Fabrication of Prototype

The sensor fabrication process was carried out at the University of Illinois at Chicago. The step-by-step description of the fabrication process of the prototype sensors is presented below. These sensors measure 25 mm by 8 mm.

1. Using AutoCAD 2002, an appropriate template was created to design an appropriate rigid reservoir. In addition, a 100W CO2 laser manufactured by *Universal Laser Systems* allowed us to selectively weld the two films together. This ensured an appropriate set of fluid channels which could guide draining solution into the rigid reservoir.

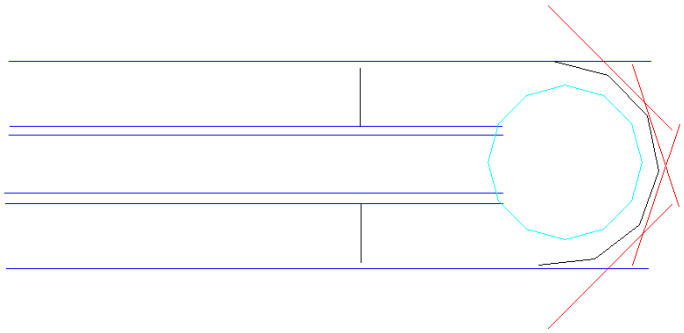

Fig. 4: Template AutoCAD Design for the Mylar Film; By Kasun Punchihewa

2. Excess Mylar film is trimmed from around the sensor and a 0.5 mm diameter LDPE tube with a length of 30 cm is inserted into the center channel.
3. The ends of the electrode sensor are placed into the outer edges of the newly designed rigid reservoir. They are then sealed of using acrylic strips and glue. With a small amount of exposed electrode left, it allows for us to run the measurements using those ends.
4. Approximately 0.135 ml of saline solution is inserted through the LDPE tube using a medical syringe. Care is taken to ensure no air pockets form inside of fluid sack, and the LDPE tube is sealed shut.

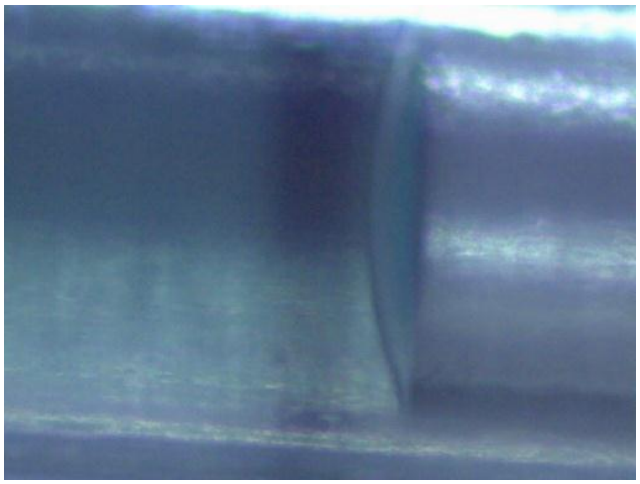

Fig. 5: 200x Magnification of center of prototype pressure sensor. The compliant fluid (saline) that is flowing in the center LDPE tube is located in the center of the image.

Part II: Experiment

The testing is set to be performed in-vitro and it gets carried out by the use of a custom built acrylic vacuum chamber with dimensions of 120 mm in length and 80 mm in height and width. Once the sensor is placed in, it is sealed in the airtight box by screwing it on top with a cover. Also, the two ends of exposed electrodes are wired and then connected to an Inductance Analyzer. We place the device down in a horizontal manner to avoid other miscellaneous forces during our experiments as well as to avoid the extra work the sensor may have to subdue if placed vertically. The chamber is connected to a small aquarium pump, and an adjustable valve is connected in between the pump and the chamber.

After turning on the aquarium pump, the valve is slowly opened allowing pressure to build up in the chamber. The pressure gauge displays the gauge pressure that is applied to the sensor. Once the pressure inside of the chamber reaches a desired value the valve is closed. In our case, we ranged the pressure from 0 to 50 inches in water. Once the fluid is at a state of equilibrium, we record the volume of fluid drained from sensor, the impedance, and the gauge pressure. This process is continued from atmospheric pressure to 50 inches in water above atmospheric pressure. The process is then reversed to arrive back at atmospheric pressure by slowly bleeding pressure out of the vacuum chamber and taking the measurements of impedance accordingly. In addition, we conducted a similar test to see how the conductivity varied during the change of pressure increase and decrease.

The last part of our experiment consisted of placing the pressure sensor under various salt concentrations to see whether or not the impedance varied significantly.

Naturally speaking, the saline when interacting with such electrolytes as salt should only essentially detect and counter it but not influence the body-like parameters. We tested this concept by selecting various amounts of salt from 1, 3, 5, 10, 15, and 20 g of salt. We kept the volume constant throughout by using only 400 mL of DI (de-ionized) water. The salt concentration densities [in grams/milliliter or g/mL] are therefore the following amounts: 0.0025 g/mL (for the 1g of salt), 0.0075 g/mL (for the 3g of salt), 0.0125 g/mL (for the 5g of salt), 0.025 g/mL (for the 10g of salt), 0.0375 g/mL (for the 15g of salt), and 0.05 g/mL (for the 20g of salt). The time frame that was implemented was from 0 to 3 minutes which was noted down in seconds because the recording occurred in 30 second intervals.

Fig. 6a - d: Schematic and pictures of the experiment.

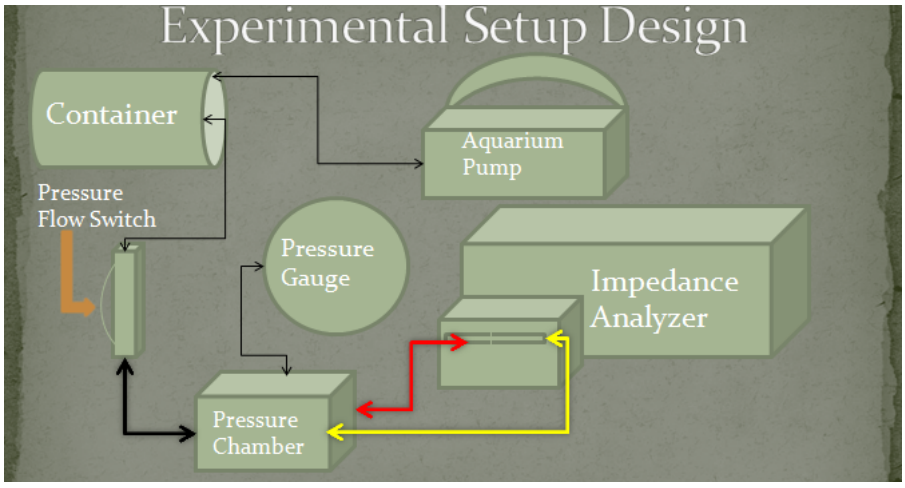

Fig. 6a: Schematic of the experimental setup used

Fig. 6b: Picture of the Experimental Setup Part I for Impedance vs. the Total Pressure

Fig. 6c: Picture of the Experimental Setup Part II for Conductivity vs. the Total Pressure

Fig. 6d: Picture of the Experimental Setup Part III for Impedance vs. Time at Various Salt Concentrations

Part III: COMSOL Modeling

The other part of this project was to run simulations through the software known as COMSOL. This modeling software allows the user to better predict and receive feedback with appropriate initial analysis regarding the mechanical properties of the model implanted based on the materials and dimensions indicated. In this case, the capacitive MEMS pressure sensor model had been considered in order to better understand and justify some of the designs being implemented upon our prototype. The testing occurs in correspondence with the materials and constraints considered prior to running the simulations. It currently has been only used as a means of justification for seeing how effective a sensor can withstand various mechanical properties. The specific stress being considered here is the von Mises stress. The von Mises stress is summarized as the maximum stress that occurs at a particular point in an object under load, while the yield point is where a material begins to deform plastically[7]. Keeping this in mind, there may be a possibility for the von Mises stress well below the yield point but this has not been shown directly. Figures 7 and 8 both indicate the process of this through their simulated results. The capacitive pressure sensor 2D model (Figure 7) specifically measures the mechanical properties through the von Mises stress and sensor deformation based on the change of ambient pressure. It also simulates how the electrical field lines would flow through the material before receiving any sort of resistance or interference. The capacitive pressure sensor 3D model (Figure 8) specifically measures the sensor deformation and von Mises stress based on the ambient pressure simulated. We are still trying to determine an appropriate and reliable means by which this process can be

implemented with the constraints of the biocompatible materials that we are currently using to run the appropriate simulations in correspondence with our prototype.

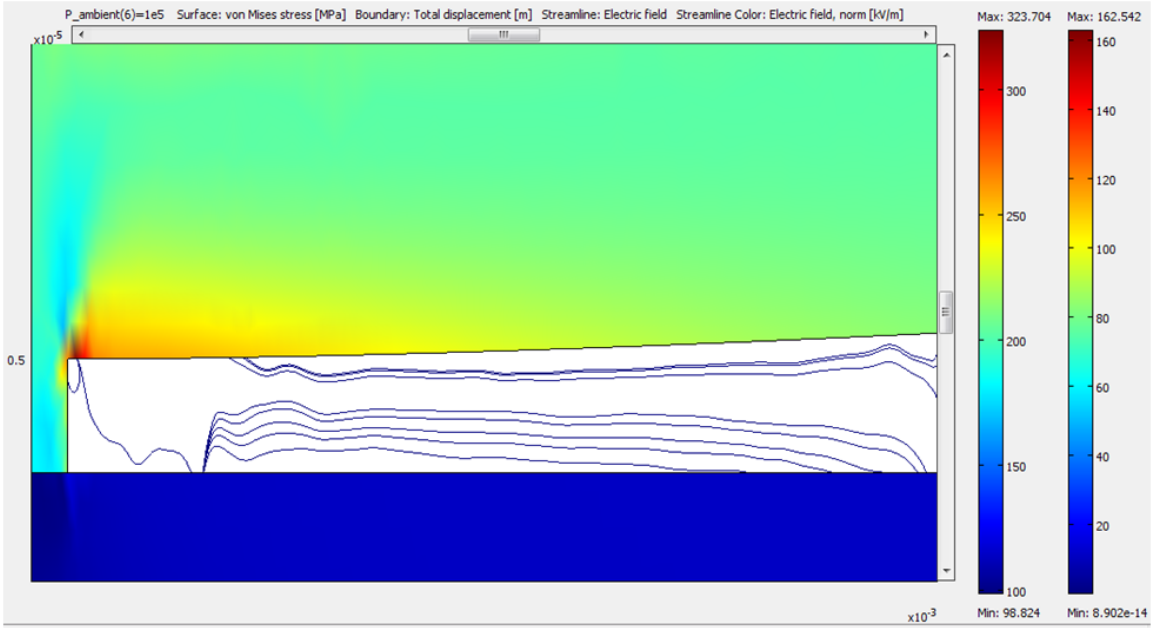

Fig. 7: Picture of the COMSOL Simulation of a Capacitance MEMS Pressure Sensor Model in 2-D; Images courtesy from COMSOL Multiphysics and COMSOL AB™

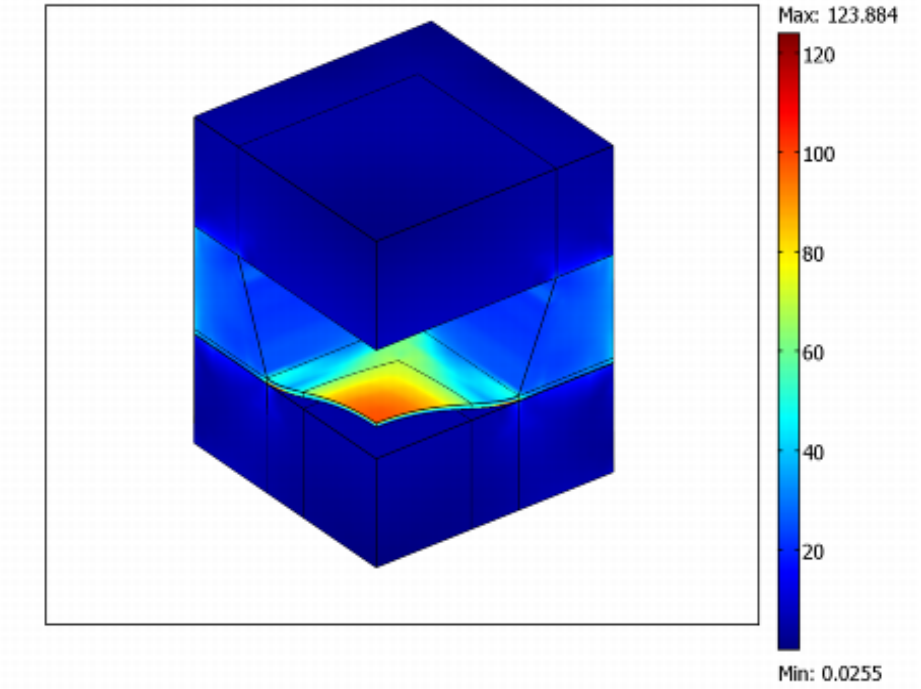

Fig. 8: Picture of the COMSOL Simulation of a Capacitance MEMS Pressure Sensor Model in 3-D; Images courtesy from COMSOL Multiphysics and COMSOL AB™

Results

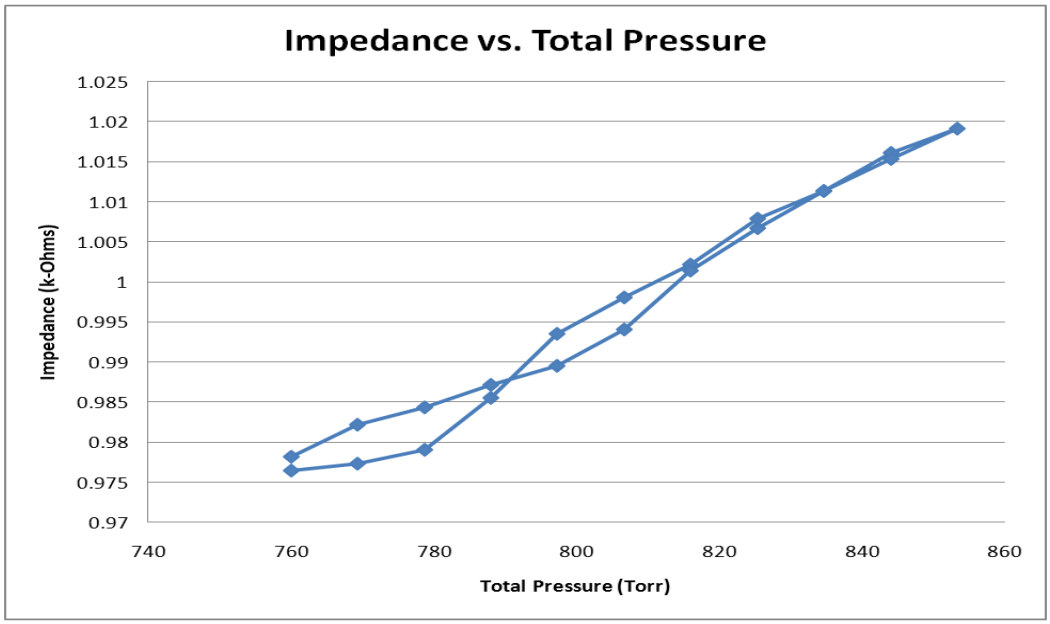

Fig. 9: Electrical impedance in kilo-Ohms versus Total pressure in Torr.

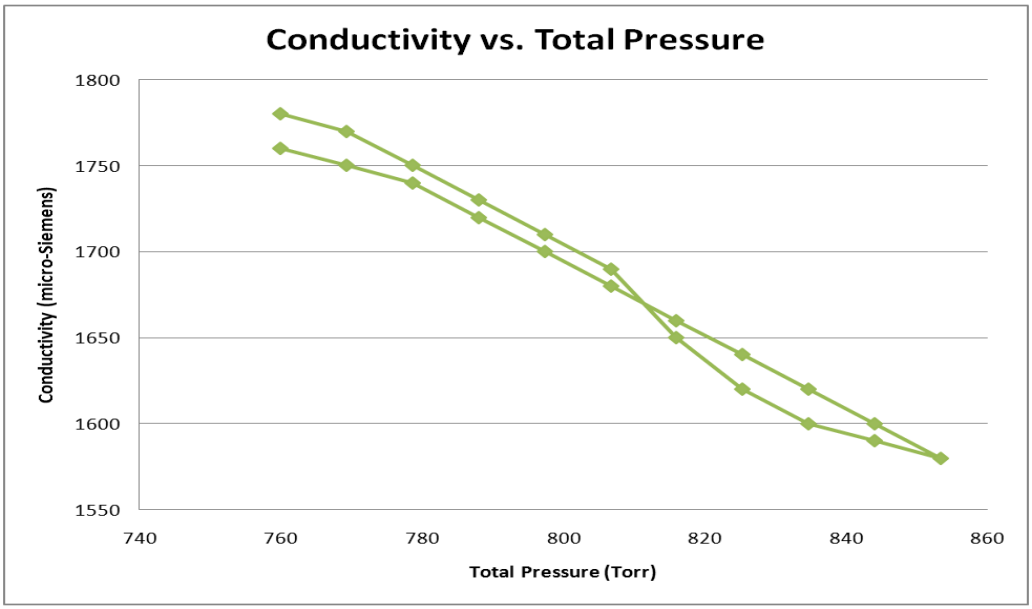

Fig. 10: Electrical conductivity in micro-Siemens versus Total pressure in Torr.

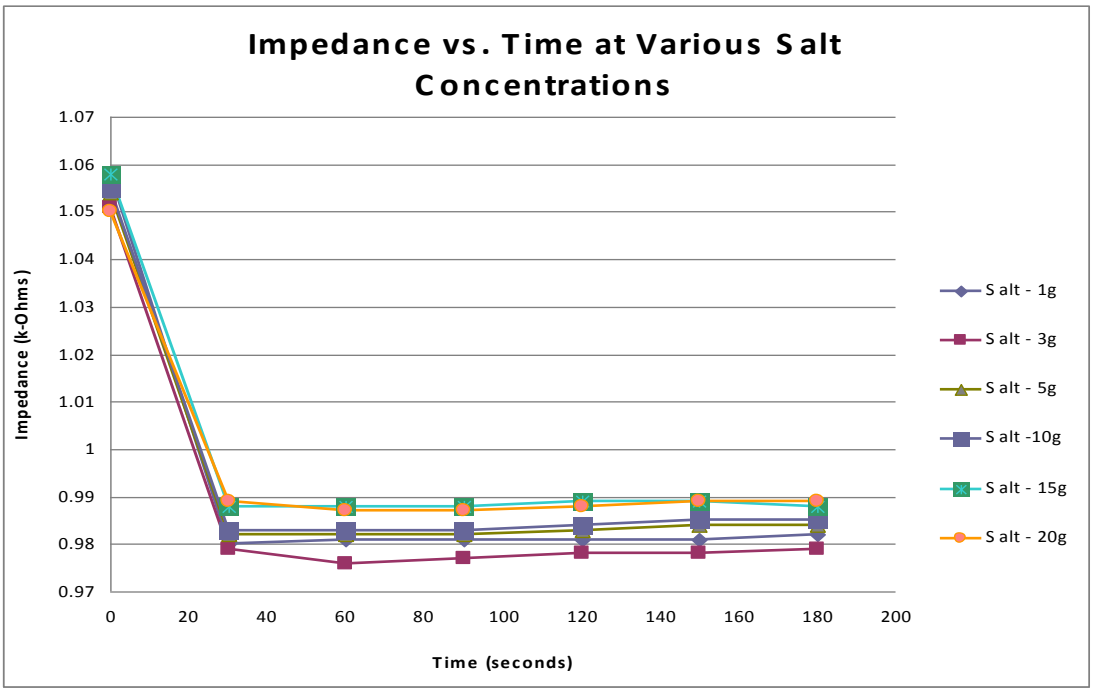

Fig. 11: Electrical impedance in kilo-Ohms versus Time in seconds. ***Constant volume of 400 mL of DI water used for each salt amount shown above.****

The following trends appeared accordingly as described in the following manner. Figure 9 measured the variation of the electrical impedance in kilo-Ohms as the pressure varied from 760 Torr and returned back to 760 Torr at the end. This has been noted as the total pressure (defined as the amount of pressure in the closed system + 760 Torr). It is important to note that the pattern the pressure was changed was by increments of 5 till it reached 853.4 Torr and then it decrements by fives till it reaches 760 Torr. As seen, the electrical impedance starts from around 0.977 kilo-Ohms and returns back to 0.978 kilo-Ohms. The relationship happens to show a direct correlation between impedance versus pressure experimented through this first phase.

Next, Figure 10 measured the variation of the electrical conductivity in micro-Siemens as the pressure varied from 760 Torr and returned back to 760 Torr at the end. The pressure of course being noted as the total pressure mentioned above and the change of pressure by increments and decrements of 5 as described earlier. In this situation however, the readings show that there is a start of conductivity around 1760 micro-Siemens at first but it starts to decrease until it reaches the midway point at which it starts to rise back up until you return back to 760 Torr at which the conductivity is approximately 1780 micro-Siemens. This correlation shows an indirect proportional relationship between the conductivity versus pressure as tested through Part II of the experimental phase.

Finally, Figure 11 measures the variation of the electrical impedance again in kilo-Ohms versus the time the sensor undergoes exposed to a specific salt concentration. The labels indicate a certain amount of salt used so that the reader knows what amounts were used precisely. The volume of the DI water remained constant at 400 milliliters. As

mentioned earlier, the salt concentration densities [in grams/milliliter or g/mL] are: 0.0025 g/mL (for the 1g of salt), 0.0075 g/mL (for the 3g of salt), 0.0125 g/mL (for the 5g of salt), 0.025 g/mL (for the 10g of salt), 0.0375 g/mL (for the 15g of salt), and 0.05 g/mL (for the 20g of salt). We noticed that the impedance readings stayed around 0.98 kilo-Ohms throughout all six concentration variations even after a whole period of being exposed for 3 minutes in the simulated ionic solution. As noticed earlier, the final electrical impedance after our test from Figure 9 was also around 0.98 kilo-Ohms as well. The value of the final reading from Figure 9 should have corresponded with the readings overall in Figure 11. This happened to be the case. This consistency was important to notice because it is important to consider how well the sensor will function based on ionic solutions in the bloodstream and also for how long of a period in time. Overall, each of these tests have played a role in helping better analyze the properties and resourcefulness for the prototype to potentially ready for the future medical in-vivo research and testing.

Discussion

Overall results indicated an appropriate trend as predicted between the impedance vs. total pressure, conductivity vs. total pressure, and impedance vs. time at various salt concentrations. Once again, keep in mind that the COMSOL simulations were only performed to better understand the mechanical properties analyzed through the software for the pressure sensor model. It provides a means of justification for the time being. The first results were suggested to be related in a direct proportional correlation which occurred as the pressure increases so does the impedance and as the pressure decreases so does the impedance. The next results were suggested to show an indirect proportional

relationship which occurred as the pressure increased the conductivity decreases and as it decreases the conductivity increases. The final experiment performed allowed for us to understand whether the impedance readings would remain consistent over time under various salt concentrations. The reason this was performed was to better understand the ionic fluctuations that take place in the body constantly especially throughout the blood stream. We were hoping the pressure sensor readings would not fluctuate significantly during our test. This happens to carry out during our runs.

One thing to note was that there is a huge jump at first before the consistent trend occurs from the results in Figure 11. We believe this may have occurred due to the sensor's exposure to the air prior to the start of this experiment and potential interference of hydrostatic pressure as a result when submerged into the beaker. Some possible errors and situations that have occurred during our experimentation were the designing of the sensors. This process is very crucial and even the slightest error can prevent the sensor from functioning accordingly. Also, it is important to check that the mylar film being used does not have extraneous tears or cuts aside from the laser welding which keeps the sensor design in place and together. Further analysis still remains and more data trials are needed to help further understand the current designs that we are studying yet.

Acknowledgments

I would like to thank the following people: Dr. Alan Feinerman, Kasun Punchihewa, Naweed Paya [REU 2008 Student], and Andrew Duffy [REU 2009 Student]. Each of these people helped make my current project possible. The previous REU students provided the backbone and understanding to further a specific direction that these sensors could be implemented towards in the field. I would like to thank Kasun for his time and

availability to help explain and further my understanding and interest in this project and experimentation. Finally, I would like to thank Dr. Alan Feinerman for providing his guidance and time as well as having provided me with an opportunity to work with his research team as an intern for the NSF REU program [sponsored thru NSF(EEC-NSF Grant # 0755115) and DOD ASSURE] on an amazing project with great potential and experience towards my future career and degree(s) as a bioengineer.

References

1. A. Duffy, Kasun Punchihewa, and A. Feinerman, “Development of a Meso-scale Drift-free Pressure-sensor for Glaucoma Patients” *Journal of Undergraduate Research* – NSF REU 2009 <http://www.uic.edu/labs/AMReL/NSFREU2009/reports/JUR_REU_Final_Report_Andrew.pdf>.
2. Paul, A., Nadimpalli, S., Lin, A., Hsu, Y., "Detailed Model of Blood Flow in the Arms and Legs Using Circuit Analysis." UIC-LPPD-112009, Nov., 2009 < http://vienna.bioengr.uic.edu/reports/coursereports.html>.
3. Bélanger MC, Marois Y. Hemocompatibility, biocompatibility, inflammatory and in vivo studies of primary reference materials low-density polyethylene and polydimethylsiloxane: a review. J Biomed Mater Res. 2001;58(5):467-77. Review.
4. N. Paya, Tatjana Dankovic, and A. Feinerman, “A Microfluidic Mixer Fabricated From Compliant Thermoplastic Films,” *Journal of Undergraduate Research* 2, pp. 1-5 (2008). http://jur.phy.uic.edu/issue2/JUR-REU0801005.pdf
5. Quigley HA, Broman AT. The number of people with glaucoma worldwide in 2010 and 2020 Br J Ophthalmol. 2006 Mar;90(3):262-7.
6. Burt K, Freeman S. Glaucoma Valves. Brown University of Biomedical Engineering. Spring 2006. http://biomed.brown.edu/Courses/BI108/2006-108websites/group02glaucoma/glaucoma.html
7. von Mises, R. (1913). *Mechanik der Festen Korper im plastisch deformablen Zustand.* Göttin. Nachr. Math. Phys., vol. 1, pp. 582–592.